DECOUPLING OF NITROGEN AND OXYGEN IMPURITIES IN NITROGEN DOPED SRF CAVITIES*

H. Hu†, Y.-K. Kim, University of Chicago, Chicago, IL, USA
D. Bafia, Fermi National Accelerator Laboratory, Batavia, IL, USA

Abstract

The performance of superconducting radiofrequency (SRF) cavities is critical for enabling the next generation of efficient high-energy particle accelerators. Recent developments have focused on altering the surface impurity profile through *in-situ* baking, furnace baking, and doping to introduce and diffuse beneficial impurities such as nitrogen, oxygen, and carbon. However, the precise role and properties of each impurity are not well understood. In this work, we attempt to disentangle the role of nitrogen and oxygen impurities through time-of-flight secondary ion mass spectrometry using niobium cavity cutouts baked at temperatures varying from 120-800 °C with and without nitrogen injection. Understanding the underlying mechanisms behind these impurities will drive further optimization in the tailoring of nitrogen and oxygen profiles for high-performance SRF cavities.

INTRODUCTION

Improving the performance of superconducting radiofrequency (SRF) cavities is the key to enabling the next generation of particle accelerators such as the International Linear Collider (ILC) or the 8 GeV Booster Replacement Linac at Fermilab [1, 2]. Two key performance metrics are quality factor (Q_0) and accelerating gradient (E_{acc}). Q_0 is inversely proportional to power loss in a cavity, so higher Q_0 cavities will lower operating costs and helium expenses [3]. High E_{acc} in cavities increases the magnitude of the kick provided to a particle, making an accelerator more efficient per unit length and lowering the cost of building a future accelerator. The performance of the SRF cavity depends primarily on the composition of the rf layer, which includes the first 100 nm of the surface, through which superconducting currents can penetrate [4]. One of the main culprits which limits SRF cavity performance has been hydrogen; the presence of hydrogen impurities in the rf layer leads to the precipitation of highly lossy niobium hydrides and nanohydrides on the surface [5–7]. Many studies have been conducted on the development of surface treatments to minimize these prohibitive effects through the introduction and diffusion of impurities such as oxygen and nitrogen [8–11].

One such treatment is nitrogen doping: a state-of-the-art high Q_0 treatment that enabled the construction of LCLS-II [12, 13]. Nitrogen doping introduces uniform and dilute concentrations of nitrogen into the rf layer [8]. A key performance feature of a N doped cavity is the anti Q-slope, an increase in Q_0 with increasing E_{acc}, which typically occurs at E_{acc} below 20 MV/m [8]. While there are some theories which propose the cause of anti-Q slope, there is no general consensus on which underlying mechanisms are responsible for it [14–17]. One theory is that nitrogen impurities act as a trap for interstitial hydrogen, preventing the precipitation of niobium hydrides [18].

The presence of interstitial oxygen in the Nb lattice has also been shown to reduce the precipitation of lossy niobium hydrides [18]. Recent work from E. Lechner and D. Bafia have highlighted the role of diffused oxygen in improved SRF cavity performance [19–21]. A new surface treatment termed oxygen doping (200°C *in-situ* baking) displays high Q performance by yielding an approximately uniform concentration of oxygen in the surface without completely removing the oxide [19]. The performance of the O doped cavities exhibit the anti-Q slope, a characteristic feature of N doped cavities [23, 25]. Given the similarities in performance, it has been proposed by D. Ford and P. Koufalis, among others, that impurities in the surface layer of N and O doped cavities perform similar functions in mitigating sources of loss [18, 24]. D. Ford has shown through first principle calculations that Nb will preferentially bond to O and N over H, with binding energies of -7.02 eV, -7.39 eV, and -2.41 eV, respectively [18]. In this work, we correlate the concentration of impurities, specifically N and O, to SRF cavity performance.

EXPERIMENTAL METHOD

Nb cavity cutouts from cavity TE1AES008 and an array of single-cell TESLA shaped 1.3 GHz Nb cavities were treated with the following treatments: Electropolishing (EP), 2/0+5 N-doped, Low Temperature Baking (LTB) at 120°C, and O doping at 200°C. Each cutout and cavity was subjected to the same baseline treatment of 800°C degas and 40 um EP. Between treatments, cutouts would receive between 10 um and 30 um EP to reset the surface. The specifics of each treatment are presented in Table 1.

The cutouts were analyzed with time of flight secondary ion mas spectrometry (SIMS) to obtain depth profiles of the impurities present in the Nb lattice. Each reported impurity depth profile is taken as the average of three 200 μm x 200 μm locations on each sample. The sputter crater for each spot is 600 μm x 600 μm to avoid edge effects, and the sputtering energy for the Cs ion beam is 2 keV. Vacuum was maintained at $< 4 \times 10^{-10}$ mbar in the analysis chamber and 10^{-7} mbar in the heating chamber. Cutouts

* WORK SUPPORTED BY THE FERMI NATIONAL ACCELERATOR LABORATORY, MANAGED AND OPERATED BY FERMI RESEARCH ALLIANCE, LLC UNDER CONTRACT NO. DE-AC02-07CH11359 WITH THE U.S. DEPARTMENT OF ENERGY.
† hannahhu@uchicago.edu

Table 1: Treatment process history for cavity cutouts and 1.3 GHz single-cell SRF cavities.

Cavity	Steps		
TE1AES010	EP baseline		
TE1AES010	120°C × 3 hrs *in-situ*	+120°C × 3 hrs (total 6 hrs) *in-situ*	
TE1PAV009	120°C × 48 hrs *in-situ*		
TE1AES017	200°C × 1 hr *in-situ*	+200°C × 10 hrs (total 11 hrs) *in-situ*	
TE1AES021	200°C × 20 hr *in-situ*		
TE1AES024	800°C × 3 hrs UHV	2 min N inj at 25 mTorr	5 μm cold EP

were analyzed alongside implanted N and O standards to calibrate relative SIMS intensity to concentration [26]. O^- and NbN^- signals were used to determine the relative sensitivity factor (RSF) for O and N respectively. Experimentally determined RSF values relative to the Nb were found to be 3.66×10^{21} ions/cm^3 for N and 2.11×10^{20} ions/cm^3 for O.

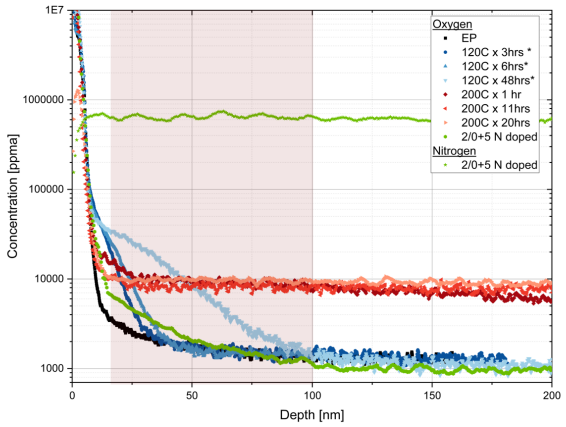

Figure 1: SIMS depth profile for absolute concentrations of N and O in Nb cavity cutouts. Concentration for starred (*) measurements were not measured directly and are scaled to the background EP baseline measurement.

Figure 1 contains the absolute concentration for each of the treatments on cavity cutouts. When available, RSF was acquired from standards during the same measurement session. If not, concentrations were scaled to background signal of the EP baseline. Baking at 120°C gradually dissolves oxygen into the bulk with a diffusion length of 40—100 nm [19]. *In-situ* baking at 200°C introduces a uniform concentration of O in the rf layer. No N was measured in the any of the EP 120°C, or 200°C baked cavity cutouts. Nitrogen doping yields a uniform concentration of N in the rf layer, and its O concentration is comparable to that of the baseline EP O profile. This suggests that the presence of O in N doping is negligible, and we can effectively decouple N and O.

Cavity cutout results are then compared to SRF cavity performance of single-cell TESLA shaped Nb cavities of resonant frequency 1.3 GHz subjected to the same treatments in Table 1. For *in-situ* treatments, the cavities were fully assembled after EP and prior to baking. Vacuum was maintained after during testing and baking to prevent the surface oxide from regrowing. Cavities were tested at the Fermilab Vertical Test Stand (VTS) to find Q_0 vs. E_{acc} at 2 K and <1.5 K in continuous wave (CW) operation. Cooling followed the fast cool down protocol to minimize the possibility of trapping magnetic flux [19].

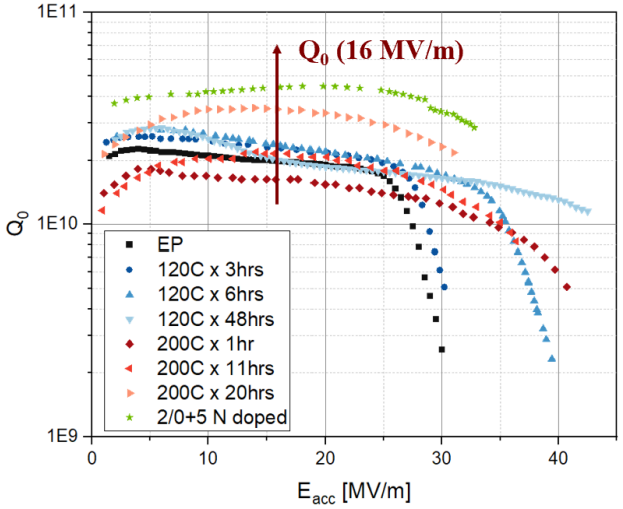

Figure 2: Q_0 vs E_{acc} performance for single-cell 1.3 GHz SRF cavities of various treatment recipes. Colors transition from darker to lighter with increased O diffusion.

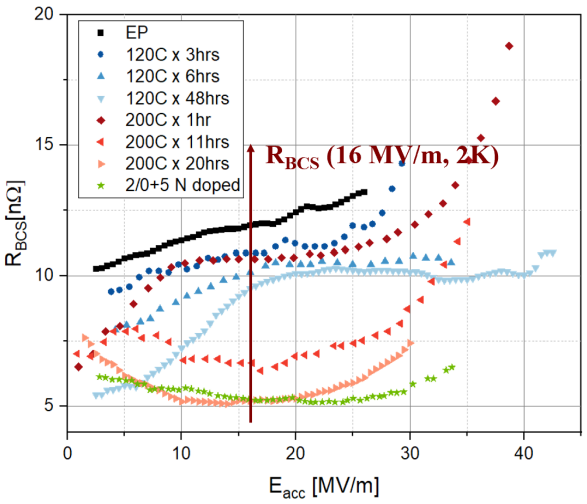

Figure 3: R_{BCS} vs E_{acc} performance for single-cell 1.3 GHz SRF cavities of various treatment recipes. Colors transition from darker to lighter with increased O diffusion.

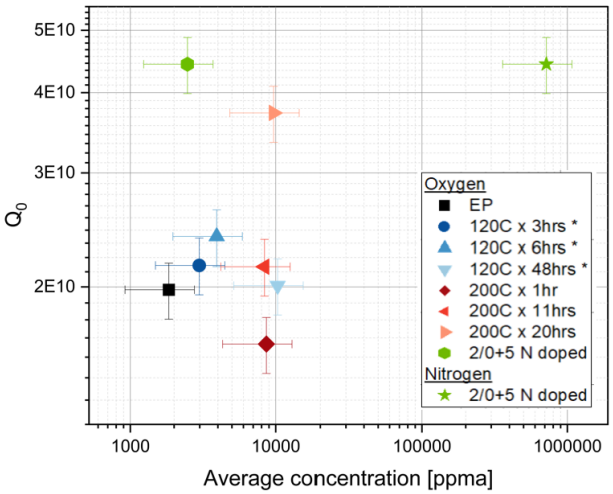

Figure 4: Q_0(16 MV/m) vs average absolute concentration of N and O.

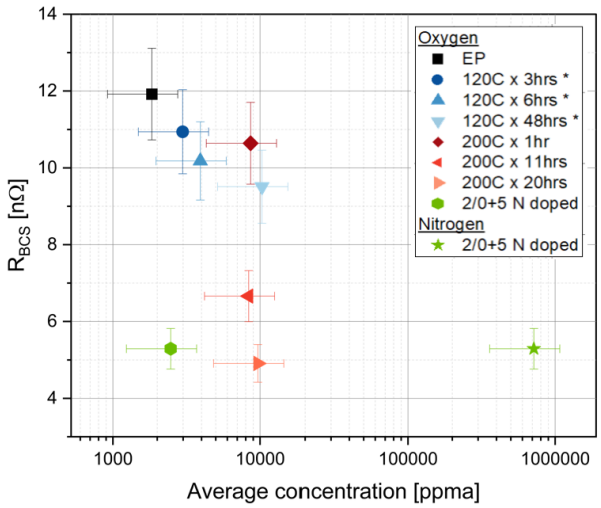

Figure 5: R_{BCS}(16 MV/m, 2 K) vs average absolute concentration of N and O.

Figures 2 and 3 shows the Q_0 and R_{BCS} performance of single-cell 1.3 GHz SRF cavities for each treatment recipe. We can see the gradual evolution towards high E_{acc} with increased 120°C baking as well as towards high Q_0 with increased 200°C baking. A decrease in R_{BCS} from longer baking and more diffused O drives the observed increase in Q_0. The performance for the O doping treatment of 200°C × 20 hrs is comparable to the high Q_0 and low R_{BCS} of 2/0+5 N doping.

RESULTS AND DISCUSSION

To correlate the results from sample cutouts and cavities, we extracted Q_0 and R_{BCS} at 16 MV/m for each of the treatments. 16 MV/m was chosen as it avoids both high field Q-slope degradation at >25 MV/m and low field (<5 MV/m) effects from surface oxides. From Fig. 1, we averaged the concentration over the first 100 nm of the surface, determined by the penetration depth of fields in Nb. The first 15 nm were excluded to consider only the concentration of dissolved O and N within the bulk.

Figure 4 correlates Q_0(16 MV/m) with the average concentration of dissolved O and N in the surface. We do not observe any distinguishable pattern since Q_0 is sensitive to both changes in the native oxide and dissolved impurities in the bulk. The concentration of N in N doped is about 2 orders of magnitudes higher than the concentrations of O from baking; the ratio of N:Nb is 0.7:1, which is much higher than expected. Further investigation is necessary to confirm this elevated concentration of N.

In Fig. 5, we correlate R_{BCS}, the quasiparticle losses from impurities within the bulk, with the average concentration of impurities in the rf layer. From a baseline R_{BCS} of 12 nΩ for EP, R_{BCS} decreases as more O is diffused into the Nb bulk. We can also confirm that the concentration of O in N doped is too low to account for the large improvement in R_{BCS} for the N doped treatment. Assuming the concentration of N is accurate, 200°C × 20 hours achieves similarly low R_{BCS} as N doped with significantly less O. Microscopically, this would suggest that O is much more effective at trapping H than N is. However, this disagrees with first principle calculations that demonstrate similar binding energies for NbO and NbN [18].

CONCLUSION

We performed material and cavity performance measurements on a number of SRF treatment recipes. We were able to decouple the effect of N and O impurities as there is no N for *in-situ* baking and negligible O for N doping. We compared the results from cavity cutouts and cavities to that as concentration of dissolved O increased, R_{BCS} decreased. With sufficient O diffusion, we can achieve a similarly low R_{BCS} as with N in N doped. In addition, it seems like significantly less O is necessary to achieve the same improvement in performance as N, suggesting that O is more effective than N at trapping H. O diffusion may be a promising technology towards the development of a next generation high Q_0 and high E_{acc} SRF cavity treatment. More studies are necessary to confirm these results.

REFERENCES

[1] D. Nueffer *et al.*, "An 8 GEV Linac As The Booster Replacement In The Fermilab Power Upgrade", arXiv, 2023. doi:10.48550/arXiv.2203.05052

[2] D. Bafia *et al.*, "Gradients of 50 MV/m in TESLA Shaped Cavities via Modified Low Temperature Bake", in *Proc. SRF'19*, Dresden, Germany, pp. 586–591, 2019. doi:10.18429/JACoW-SRF2019-TUP061

[3] H. Padamsee, J. Knobloch, and T. Hays, *RF Superconductivity for Accelerators*. Weinheim, Germany: Wiley-VCH GmbH, 1998.

[4] S. Isagawa, "Influence of hydrogen on superconducting niobium cavities", *J. Appl. Phys.*, vol. 51, pp. 6010–6017, 1980. doi:10.1063/1.327523

[5] Y. Trenikhina *et al.*, "Nanostructural features degrading the performance of superconducting radio frequency niobium cavities revealed by transmission electron microscopy and electron energy loss spectroscopy", *J. Appl. Phys.*, vol. 117, 2015. doi:10.1063/1.4918272

[6] J. Knobloch, "The 'Q disease' in Superconducting Niobium RF Cavities", in *First Int. Workshop on Hydrogen in Materials and Vacuum Systems*, vol. 671, pp. 130-150, 2003. doi:10.1063/1.1597364

[7] F. Barkov *et al.*, "Precipitation of Hydrides in High Purity Niobium after Different Treatments", *J. Appl. Phys.*, vol. 114, pp. 164904, 2013. doi:10.1063/1.4826901

[8] A. Grassellino *et al.*, "Nitrogen and argon doping of niobium for superconducting radio frequency cavities: a pathway to highly efficient accelerating structures", *Supercond. Sci. Tech.*, vol. 26, pp. 102001, 2013. doi:10.1088/0953-2048/26/10/102001

[9] A. Grassellino *et al.*, "Unprecedented quality factors at accelerating gradients up to 45 MV/m in niobium superconducting resonators via low temperature nitrogen infusion", *Supercond. Sci. Tech.*, vol. 30, 2017. doi:10.1088/1361-6668/aa7afe

[10] A. Romanenko *et al.*, "Effect of mild baking on superconducting niobium cavities investigated by sequential nanoremoval", *Phys. Rev. ST Accel. Beams* vol. 16, pp. 012001, 2013. doi:10.1103/PhysRevSTAB.16.012001

[11] S. Posen *et al.*, "Ultralow surface resistance via vacuum heat treatment of superconducting radiofrequency cavities", *Phys. Rev. Applied*, vol. 13, pp. 014024, 2020. doi:10.1103/PhysRevApplied.13.014024

[12] J. Galayda, "The LCLS-II: A High Power Upgrade to the LCLS", in *Proc. IPAC'18*, Vancouver, Canada, pp. 18–23, 2018. doi:10.18429/JACoW-IPAC2018-MOYGB2

[13] T. Raubenheimer, "The LCLS-II-HE, A High Energy Upgrade of the LCLS-II", in *Proc. FLS'18*, Shanghai, China, pp. 6–11, 2018. doi:10.18429/JACoW-FLS2018-MOP1WA02

[14] M. Martinello *et al.*, "Field-Enhanced Superconductivity in High-Frequency Niobium Accelerating Cavities", *Phys. Rev. Lett.*, vol. 121, 2018. doi:10.1103/physrevlett.121.224801

[15] B. P. Xiao, C. E. Reece, and M. J. Kelley, "Superconducting surface impedance under radiofrequency field", *Physica C*, vol. 490, pp. 26–31, 2013. doi:10.1016/j.physc.2013.04.003

[16] A. Gurevich, "Reduction of Dissipative Nonlinear Conductivity of Superconductors by Static and Microwave Magnetic Fields", *Phys. Rev. Lett.*, vol. 113, no. 8,2014. doi:10.1103/physrevlett.113.087001

[17] G. Ciovati, P. Dhakal, and A. Gurevich, "Decrease of the surface resistance in superconducting niobium resonator cavities by the microwave field", *Appl. Phys. Lett.,* vol. 104, no. 9, 2014. doi:10.1063/1.4867339

[18] D. C. Ford, L. D. Cooley, and D. N. Seidman, "First-principles calculations of niobium hydride formation in superconducting radio-frequency cavities", *Supercond. Sci. Technol.*, vol. 26, p. 095002, 2013. doi:10.1088/0953-2048/26/9/095002

[19] D. Bafia *et al.*, "The role of oxygen concentration in enabling high gradients in niobium SRF cavities", in *Proc. SRF'21*, East Lansing, MI, USA, Jun.-Jul. 2021. doi:10.18429/JACoW-SRF2021-THPTEV016

[20] E. M. Lechner *et al.*, "RF surface resistance tuning of superconducting niobium via thermal diffusion of native oxide", *Appl. Phys. Lett.*, vol. 119, pp. 082601, 2021. doi:10.1063/5.0059464

[21] E. M. Lechner *et al.*, "Oxide dissolution and oxygen diffusion scenarios in niobium and implications on the Bean–Livingston barrier in superconducting cavities", *J. Appl. Phys.*, vol. 135, 2024. doi:10.1063/5.0191234

[22] D. Bafia, A. Grassellino, and A. Romanenko, "The Anomalous Resonant Frequency Variation of Microwave Superconducting Niobium Cavities Near T_c", arXiv, 2021. doi:10.48550/arXiv.2103.10601

[23] H. Hu, D. Bafia, and Y.-K. Kim, "Evaluating the Effects of Nitrogen Doping and Oxygen Doping on SRF Cavity Performance", in *Proc. IPAC'22*, Bangkok, Thailand, Jun. 2022. doi:10.18429/JACoW-IPAC2022-TUPOTK034

[24] P. N. Koufalis *et al.*, "Effects of Interstitial Oxygen and Carbon on Niobium Superconducting Cavities", arXiv, 2017. doi:10.48550/arXiv.1612.08291

[25] D. Bafia, A. Grassellino, and A. Romanenko, "The Anomalous Resonant Frequency Variation of Microwave Superconducting Niobium Cavities Near T_c", arXiv, 2021. doi:10.48550/arXiv.2103.10601

[26] A. Budrevich and J. Hunter, "Metrology aspects of SIMS depth profiling for advanced ULSI processes", in *Characterization and Metrology for ULSI Technology*, 1998. doi:10.1063/1.56792